Kashf Journal of Multidisciplinary Research
Vol: 02 - Issue 10 (2025)
P-ISSN: 3007-1992 E-ISSN: 3007-200X
https://kjmr.com.pk

CITRIC ACID MEDIATED GREEN SYNTHESIS OF COPPER NANOPARTICLES USING CINNAMON BARK EXTRACT: STRUCTURAL CHARACTERIZATION, CATALYTIC EFFICIENCY, AND ANTIBACTERIAL APPLICATIONS

[1]Abdul Qadeer*, [2]Muhammad Fahad Hayat, [3]M Lateef , [4]Muhammad Sheeraz, [5]Muhammad Aqib Majeed, [6]Muhammad Shahbaz

[1, 2, 3, 4, 5, 6] Department of Chemistry, Ghazi University Dera Ghazi Khan.

****Corresponding Author:*** abdulqadeerchandia3344@gmail.com

Article Info

Abstract

The synthesis of copper nanoparticles (CuNPs) through eco-friendly methods has attracted significant attention as a sustainable alternative to conventional chemical approaches that rely on hazardous reagents. In this study, a novel citric acid-mediated biosynthetic route was developed using cinnamon bark extract as both a reducing and stabilizing agent. Citric acid played a dual role in enhancing the reductive capability of cinnamon phytochemicals and in controlling nanoparticle morphology, resulting in highly stable, spherical CuNPs with uniform surface roughness. The synthesized nanoparticles were characterized using UV–Vis spectroscopy, SEM, XRD, and FTIR analyses, which confirmed their crystalline structure, homogeneous distribution, and biomolecule-assisted capping. Functional assessment demonstrated remarkable catalytic efficiency, with CuNPs achieving over 80% degradation of the carcinogenic dyes methylene blue (MB) and methyl orange (MO) in the presence of sodium hypophosphite, a non-toxic reducing agent. Furthermore, antibacterial studies against Staphylococcus aureus and Escherichia coli revealed superior inhibition zones, particularly in citric acid-assisted CuNPs, underscoring their broad-spectrum antimicrobial potential. The combined catalytic and antibacterial properties highlight the versatility of these nanoparticles for environmental and biomedical applications. This green synthesis route not only eliminates the use of toxic chemicals but also offers a cost-effective and scalable strategy for producing CuNPs suitable for wastewater remediation, medical fabrics, and personal protective equipment, contributing to sustainable nanotechnology advancements.

Keywords:

Copper nanoparticles (CuNPs); Green synthesis; Cinnamon bark extract; Citric acid mediation; Nanoparticle characterization; Antibacterial activity

1. INTRODUCTION

1.1. Background and Motivation

Nanotechnology has emerged as a transformative field with wide-ranging applications in medicine, catalysis, water purification, electronics, and antimicrobial coatings. Among the different classes of nanomaterial, copper nanoparticles (CuNPs) have gained considerable attention due to their low cost, high electrical and thermal conductivity, and strong antibacterial and catalytic properties. Their utility in areas such as dye degradation, antimicrobial textiles, and biomedical devices makes them highly attractive for both industrial and societal applications. However, conventional methods of synthesizing CuNPs—including chemical reduction, thermal processing, and micro emulsion techniques—often involve hazardous reducing agents, toxic stabilizers, and energy-intensive processes. These approaches raise concerns about environmental pollution, human health risks, and unsustainable resource use, thereby creating an urgent need for greener alternatives (Jahanbakhshi & Habibi, 2016).

Green synthesis of nanoparticles, particularly through plant-based extracts, has emerged as a promising alternative because it eliminates toxic chemicals and capitalizes on the reducing and stabilizing potential of naturally occurring biomolecules. Plant extracts contain secondary metabolites, such as flavonoids, terpenoids, alkaloids, and polyphenols, which can act as bioreductants and capping agents, facilitating nanoparticle formation more safely and sustainably. Despite this promise, a major challenge persists: many plant extracts exhibit limited reduction capacity, resulting in inconsistent nanoparticle morphology, aggregation, and poor reproducibility. Overcoming this limitation remains a key motivation in advancing biogenic synthesis strategies (Esa & Sapawe, 2020).

Cinnamon bark extract has long been recognized for its rich phytochemical composition, including eugenol, cinnamaldehyde, and flavonoids, which possess strong antioxidant and antimicrobial properties. These compounds make cinnamon a promising candidate for the biosynthesis of nanoparticles. However, without enhancement, its reducing ability is often insufficient to produce stable, uniformly distributed CuNPs. To address this gap, citric acid can be introduced as a mediator. Citric acid not only enhances the reducing potential of cinnamon extract but also influences particle size, shape, and stability due to its strong antioxidant and chelating properties. The synergistic use of cinnamon and citric acid thus offers a powerful and environmentally safe approach to overcome the limitations of natural extracts alone (Singh et al., 2025).

The motivation for this study stems from two pressing global challenges: environmental pollution and antimicrobial resistance. Industrial dyes, such as methylene blue (MB) and methyl orange (MO), are persistent pollutants that contaminate water systems and pose significant health risks. At the same time, the rise of drug-resistant pathogens underscores the need for effective, non-toxic antimicrobial agents. By developing CuNPs through an eco-friendly biosynthetic route, this work addresses both issues. The synthesized nanoparticles are evaluated for their catalytic performance in dye degradation and for their antibacterial efficacy against Escherichia coli and Staphylococcus aureus.

This dual functionality positions the research at the intersection of environmental sustainability and public health. The successful demonstration of citric acid-mediated green synthesis not only provides a scalable, low-cost alternative to conventional methods but also expands the scope of CuNP applications in

wastewater treatment, antimicrobial textiles, medical fabrics, and protective equipment. Ultimately, this study is motivated by the goal of advancing sustainable nanotechnology solutions that balance high performance with ecological responsibility, offering tangible benefits for both industry and society (Luo et al., 2023).

Copper nanoparticles (CuNPs) are increasingly recognized for their multifunctional properties, which make them valuable in diverse technological and biomedical fields. As highlighted by (Baghirova et al., 2023), these applications include photocatalysis, electronic devices, thermal management systems, metalworking, and electromagnetic interference (EMI) shielding. In the medical and life sciences sector, the tunability of nanoparticle size, shape, and morphology has driven advances in biosensing, bioimaging, conductive films, disinfectants, and antibacterial treatments (Needaa et al., 2016). Such versatility has led researchers to explore numerous synthesis methods, including chemical reduction, microemulsion, polyol, thermal processing, and vapour deposition techniques (Mishra et al., 2023). Early attempts, such as those by (Abdo & Haneef, 2013) with gas vapour methods, laid the foundation, while chemical wet processing later emerged as one of the more practical approaches (Onwudiwe et al., 2020). However, despite their effectiveness, these conventional methods often rely on toxic solvents, polymers, or reducing agents, which limit their widespread adoption due to environmental and safety concerns (Salgaokar, 2023).

To overcome these limitations, attention has shifted toward green synthesis methods using biological systems. Both microbial and plant-based extracts have been explored as alternatives (Teo et al., 2019). Microorganisms can facilitate nanoparticle formation through their redox-active secretions, which reduce metal ions and promote the development of metal-protein complexes. However, microbial synthesis is often hindered by challenges such as controlling pH, temperature, and salt concentration, as well as the difficulty of separating and purifying nanoparticles (Lashari et al., 2022).

Plant extracts, in contrast, present a more practical and environmentally safe alternative. Rich in secondary metabolites such as flavonoids, terpenoids, alkaloids, proteins, and polysaccharides, plants provide natural reducing and capping agents that enable efficient nanoparticle formation. These phytochemicals not only facilitate bioreduction but also stabilize the nanoparticles, thereby preventing aggregation and enhancing their functional performance (F. Li et al., 2021). As a result, nanoparticles synthesized from plant extracts exhibit enhanced properties, making them attractive for applications in medicine, agriculture, pharmacology, and cosmetics (Benelmekki et al., 2015).

Extensive research has investigated various plant parts, including leaves, bark, stems, roots, flowers, and seeds, as bio-reductants for nanoparticle synthesis. While many studies have reported successful outcomes, a persistent challenge remains in producing uniformly distributed nanoparticles with consistent morphology. Table 1 provides a summary of earlier work on the biosynthesis of nanoparticles using various plant species, emphasizing the diversity of natural resources that can be exploited for sustainable nanomaterial production.

Table 1. Fabrication of metal nanoparticles with botanical extraction.

Nanoparticle	Plant Species	Used Part	Reference
Ag	Brassica oleracea	Fruit leaves	(Noghabi et al., 2017)
Ag	Eucalyptus oleosa	Leaf	(Kotb & M. Alabdallah, 2024)
Ag	Aloe vera	Leaf	(Arumugam et al., 2023)
Ag	Azadirachta indica	Leaf	(Gbadamosi et al., 2022)
Ag	Ipomoea pes-caprae	Leaf	(M.-C. Li et al., 2015)
Ag, Au	Cumin	Seed	(Moshirian Farahi et al., 2023)
Ag	Cinnamom zeylanicum	Bark	(Anitha Devi et al., 2025)
Au	Coccinia grandis	Bark	(Aftab et al., 2020)
Ag, Au	Lansium domesticum	Fruit	(Mathew & Juang, 2007)
Au	Coleus aromaticus	Leaf	(Justo-Vega et al., 2025)
Ag, Au	Zingiber officinale	Roots	(Swain et al., 2023)
Cu	Piper nigrum	Seeds and particles	(Sánchez-Tovar et al., 2025)
Cu	Clove	Floral buds	(Madadkhani et al., 2024)
Cu	Punica granatum	Fruit peel	(Muraro et al., 2024)
In_2O_3	Aloe vera	Leaf	(Vargas et al., 2019)
Pd	Eucommia ulmoides	Bark	(Almomani et al., 2020)
Pd	Cinnamomum camphora	Leaf	(Anand et al., 2020)
Ni	Ocimum sanctum	Leaf	(Ahamed et al., 2013)
Ni	Dioscorea	Stem & leaf	(Nayak et al., 2006)
Ni	Desmodium gangeticum	Roots	(Patade et al., 2020)
Mn	Cinnamomum verum	Bark	(Aramendiz & Imqam, 2019)

A spice and flavouring ingredient, cinnamon may be any shade of brown, from pale to deep. Its features include a spectrum of hues. It is known that this chemical is derived from the inner bark of trees in the

Lauraceous family, namely the Cinnamomum species. For a long time, cinnamon's therapeutic properties and health benefits have been recognised and appreciated. Cinnamon has been around for a very long time. According to (Ahmad et al., 2021), cinnamon aldehyde, eugenol, cinnamic acid, L-borneol, linalool, and methyl chavicol are some of the key components that contribute to its effectiveness. Numerous studies have investigated the pharmacological benefits of cinnamon, a versatile medicinal plant, and have demonstrated its potent antioxidant, anti-inflammatory, anticancer, lipid-lowering, and antibacterial properties. The medicinal properties of cinnamon have been known for ages. Many different medicinal uses for cinnamon have been documented throughout history. Cinnamon, along with herbs like clove, cumin, and piper nigrum, which have similar chemical compositions, may be used as bio-reductants to create metal nanoparticles, according to research. The presence of eugenol and cinnamaldehyde in cinnamon is responsible for its significant oxygen absorption and antioxidant properties, as stated by (Huang et al., 2019). This may be the reason why cinnamon is effective at reducing oxygen levels. While making palladium nanoparticles, (Khoiriah & Putri, 2024) investigated how changes in temperature, pH of the reaction, and quantity of cinnamon bark extract affected their size and form. When cinnamon camphora leaf extract was used to make silver and Gold nanoparticles, researchers (Wang et al., 2024) found that the nanoparticles' size and shape changed significantly. The dimensions and size of the nanoparticles showed this transformation. (Gui et al., 2025) investigated the antibacterial properties of cinnamon-derived silver nanoparticles. Recent research by Kamran and colleagues (2019) examined the photo catalytic and antibacterial capabilities of cinnamon extract-modified manganese nanoparticles. One reason copper nanoparticles have remained popular among scientists is that they are bactericidal, antibacterial, highly conductive, inexpensive, and readily available. Copper nanoparticles have been Biosynthesised by extracting phytochemicals from a broad range of plants, including Magnolia kobus, Punica granatum, Calotropis procera, Ocimum sanctum, Citrus medica, and Eucalyptus. Numerous studies (Kavitha et al., 2024) have demonstrated that the physical and chemical processes involved in biosynthetic reactions differ among various plants and research methodologies. (Zhang et al., 2024) compiled a comprehensive catalogue of plant components suitable for copper nanoparticle production. Size and shape details on the particles were included in this inventory. It was previously unknown that cinnamon verum bark, a plant extract, was used in the production of copper nanoparticles. Although a thorough investigation is not yet available, (Cheraghian et al., 2014) attempted to create copper nanoparticles using cinnamon bark extract. Although several plant extracts are used in the biological synthesis of metal nanoparticles, their reductive properties are often inadequate, therefore limiting their widespread application. The present corpus of research literature identifies several useful methods for promoting rapid reduction, including sonication, ultrasonication, microwave assistance, and chemical agents. These papers were written by (Yan et al., 2014). However, widespread adaptation is not feasible due to the precarious position of the global energy and environmental systems (Cheraghian, 2021). These additions need either a substantial amount of energy or potentially harmful reducing chemicals, or both. This is the rationale for the situation. To improve the bio-reduction efficacy of natural extracts, scientists are driven to discover more effective and environmentally friendly ways. This is because there is a growing need for environmentally friendly production of metal nanoparticles. Chemical scientists remain fascinated by copper nanoparticles due to their potent antibacterial properties. According to recent research, copper surfaces significantly reduce the coronavirus's longevity, thereby increasing the importance of copper nanoparticles (Green et al., 2019) Copper nanoparticles have gained importance as a result of this. Citric

acid served as a bioreductant, while cinnamon bark extract stabilized the copper nanoparticles that our research team successfully synthesised. The usefulness of cinnamon verum bark as a medicinal agent, combined with the significance of copper nanoparticles, enabled this to be achieved. In addition to enhancing cinnamon's blood sugar-lowering effects, citric acid alters the particle size and shape and is an effective free radical scavenger. By using sodium hypophosphite (SHP), the levels of methyl orange (MO) and methylene blue (MB) were significantly reduced, facilitating the examination of the nanoparticles' catalytic characteristics in their as-synthesised form. In addition, our scientific inquiry did not include another sustainable component: the use of SHP as a non-toxic reductant in the chemo-catalytic breakdown of hazardous dyes. Fabric samples were subjected to further testing to see if Biosynthesised nanoparticles effectively inhibited bacterial growth. Developing a stable nanoparticle with disinfection capabilities could have a significant impact on the fight against COVID-19 and other pandemic crises. Since it contains no potentially harmful ingredients, this nanoparticle is safe for use on fabrics.

1.2. Contributions of the study

Novel Green Synthesis Approach:

- Developed a simple, eco-friendly, and one-step method for synthesizing copper nanoparticles (CuNPs) using cinnamon bark extract.
- Introduced citric acid as a mediator, which significantly enhanced the reducing ability of cinnamon phytochemicals and improved nanoparticle morphology.

Enhanced Nanoparticle Properties:

- Achieved uniform, spherical CuNPs with stable surface roughness, overcoming the common limitation of poor uniformity in biogenic synthesis.
- Demonstrated that citric acid plays a dual role—acting as a reducing enhancer and a stabilizer—resulting in improved nanoparticle distribution.

Comprehensive Characterization:

- Confirmed nanoparticle formation and properties using UV–Vis spectroscopy, SEM, XRD, and FTIR, providing evidence of crystalline structure, surface capping, and biomolecule interaction.

Catalytic Efficiency:

- Demonstrated strong catalytic performance in degrading hazardous dyes (methylene blue and methyl orange), achieving >80% removal efficiency.
- Highlighted sodium hypophosphite (SHP) as a safer alternative to sodium borohydride, making the catalytic process more environmentally sustainable.

Antibacterial Activity:

- Showed significant antibacterial effects against Escherichia coli and Staphylococcus aureus.

- Citric acid–mediated CuNPs exhibited larger inhibition zones, proving superior antimicrobial potential compared to cinnamon-only CuNPs.

Sustainable and Scalable Method:

- Eliminated the use of hazardous chemicals, solvents, and polymers commonly used in nanoparticle synthesis.
- Presented a cost-effective and scalable strategy suitable for industrial applications.

Practical Applications:

Demonstrated that the synthesized CuNPs can be used in:

- Wastewater treatment (dye degradation)
- Medical fabrics and PPE (antimicrobial coatings)
- Environmental disinfection (broad-spectrum antibacterial use)

Highlighted their relevance in addressing global challenges such as water pollution and antimicrobial resistance, with potential implications for pandemic preparedness.

2. Experimental

2.1. Materials and methods

Sigma Aldrich, the corporation in question, was the go-to source for copper nitrate. Agar, sodium hypophosphite (SHP), citric acid, and anhydrous citric acid (CA) were sourced from Daejung Chemicals in Korea. We also bought ammonia water. All the dyes used in this experiment, including methylene blue (MB) and methyl orange (MO), were sourced from Sigma-Aldrich. We did not purify any of the compounds before using them; instead, we utilized them as-is. For our cinnamon bark buy, we shopped at one of the local internet food stores.

2.2. Characterizations

The nanoparticles' surface Plasmon resonance effect and catalytic efficacy were assessed using an Agilent Technologies Cary Series ultraviolet-visible-near-infrared spectrophotometer. Investigating the surface morphology was accomplished using a JEOL 7500F field-emission scanning electron microscope (FE-SEM). We used a Bruker D8 FOCUS X-ray diffractometer to analyses the crystal structures of the samples and determine their phase composition. The instrument was configured to run at an accelerating voltage of 40 kV and a current of 40 mA. From approximately 10 degrees to 80 degrees, the diffract meter could measure a wide range of angles. The diffractometer, equipped with CuKα radiation, reported a λ value of 1.5418 Å. The Nicolet iD5-ATR spectrophotometer was used in combination with the disc diffusion test equipment to acquire the infrared spectra. The efficacy of antibacterial medicines was assessed using a disc diffusion experiment.

2.3. Cinnamon Extract Preparation Procedures

Following the traditional process for cinnamon manufacture, the bark was first washed extensively with deionized water to eliminate any surface contaminants. It was then pounded into a grainy powder after being let to dry naturally in the air. Ten grams of powdered cinnamon was added to 100 millilitres of deionised water in a round-bottomed flask. Then, for forty minutes, it was heated to the boiling point by connecting the reaction vessel to a condenser that was cooled by water. To prepare the mixture for use, it was passed through two layers of Whatman filter paper (No. 1), with the first layer serving as a filter. Before starting the refluxing procedure, ensure that the glassware is cleaned with detergent-free water and ethanol.

2.4. Preparation of copper nanoparticles

In a glass beaker, thirty millilitres of copper nitrate solution (0.1 mM) and three millilitres of cinnamon extract solution (CES) were mixed to produce copper nanoparticles (CuNPs). We divided the reaction mixture into three equal portions, each containing ten millilitres. We then used ammonia water as needed to adjust the pH of the solutions to 3, 7, and 11. The reaction solutions were subjected to constant agitation at a speed of 700 revolutions per minute and heated to 90°C to detect a colour change. The gathered samples were then subjected to UV-Vis spectroscopy. In the ultraviolet-visible band, namely between 570 and 620 nanometers, copper nanoparticles absorb the most light. You may find the peak intensities near the centre of the spectrum. An extraordinary condition of pH is indicated when a reaction solution shows a tiny peak within a given wavelength range. This demonstrates that the answer is suitable for inclusion in ongoing research projects. The optimal concentration of bio-reductant needed to form copper nanoparticles was determined by combining various volumes of cinnamon extract solutions (1, 2, 3, 4, and 5 mL) with copper salt solutions (0.1 mM) in a total volume of 10 mL, all at an appropriate pH. This ensured that the bio-reductant concentration in the solution was just right. The correct dosage of bio-reductant needed to be determined, hence this experiment was conducted. The samples were examined using the UV-visible absorption spectra. According to Table 2, the formulation was further optimised after adjusting the CES amount by increasing the reaction fluid with citric acid (4 millilitres of CES at a pH of 11). Figure 1 also provides a schematic representation of the method, illustrating the flow of the entire synthesis process.

Table 2. Experimental design for the production and improvement of copper nanoparticles.

Sample ID	Copper Precursor	Bio Reductant	Citrated Enhancer	pH	λ_{max}	Remarks
	Copper Nitrate (mM)	Cinnamon Extract (ml)	Citric Acid (%)			
S1	0.1	1	–	3	–	No peak.
S2		1	–	7	–	No peak.

S3	1	–	11	611	Small broad peak indicating the reduction.
S4	2	–	11	607	Broad peak with relative high absorption.
S5	3	–	11	591	Narrow peak with more absorption.
S6	4	–	11	589	More distinct peak with relative high absorption.
S7	5	–	11	603	Broadening of peak.
S8	–	1	11	613	Broad spectrum line with no distinct peak.
S9	4	1	11	606	District, narrow peak with relative low absorption.
S10	4	2	11	588	More absorption but peak become broader.
S11	4	3	11	587	Distinct and narrow
S12	4	4	11	588	Constant behaviour
S13	4	5	11	586	Constant behaviour

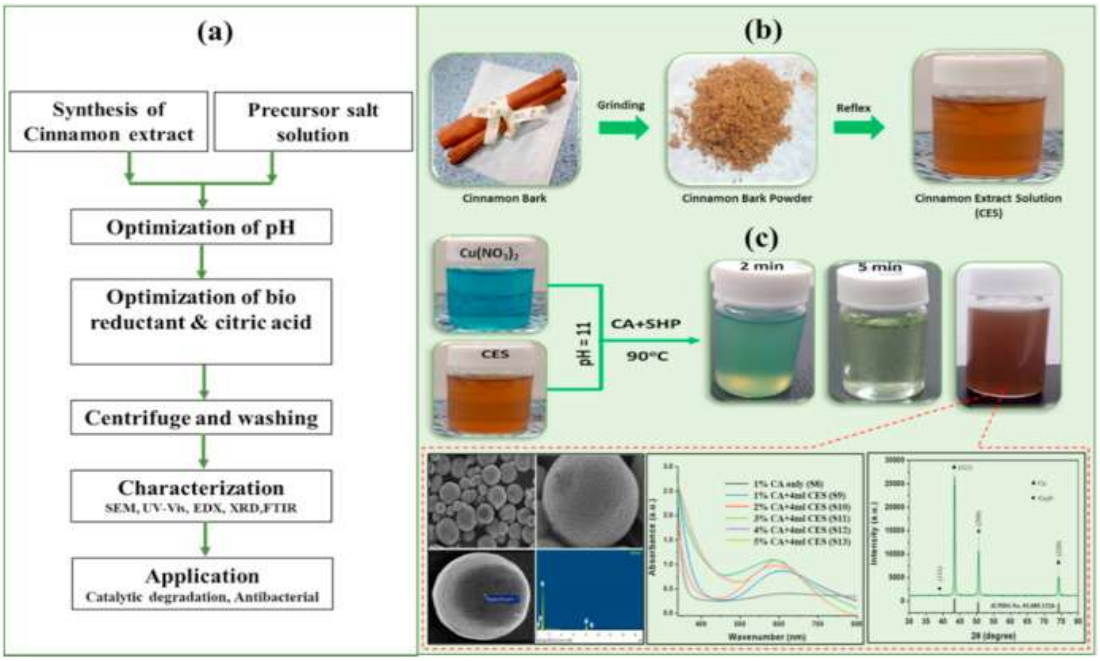

Fig.1. Schematic representation of biosynthesis: (a) process sequence diagram, (b) the production of the extract of cinnamon via solution, (c) synthesis and characterization of synthesized copper nanoparticles (CuNPs).

3. Results and Discussion

3.1. Synthesis of CuNPs

A comprehensive series of studies was conducted to create stable, biologically reduced copper nanoparticles (Table 2) the copper salt solution was first pH-balanced with one millilitre of CES added at three, seven, and eleven points. The reaction mixture changed from a turquoise blue to a greenish-blue, then to a light yellow, and finally to a brown hue over the course of 3.5 hours of continuous heating and stirring. This happened during a period of constant stirring while the mixture was heated. The pH level of the mix might be determined by observing the colour shift. Many people use cinnamon bark in their cooking and medicine due to the numerous health benefits it is known to provide. You can obtain it at a fair price, and it is readily available. Premkumar et al. (2018) found that the hue change occurs during the production process of copper nanoparticles due to the presence of bio-reducers such as eugenol, linalool, and methyl chavicol. When these compounds are added, a change in hue occurs. One method used to confirm the creation of nanoparticles is UV-Vis spectroscopy. The surface plasmon resonance effect is crucial to this method. Once the colour shift was stabilized, a peak at 611 nm was observed in the UV-Vis absorption spectrum of sample 3 at pH 11, as shown in Table 2 and Figure 2a. It was in this sample that this peak was seen. The stability of the colour change was the next step once this procedure was completed (Liu et al., 2014). At pH 7 (sample S2), a redshift and peak widening were observed, and at pH 3 (S1, Table 2, Fig. 2a), these alterations almost plateaued. Using sample S2, this was noted. According to Choudhary et al. (2018), a pH value of 11 was used in subsequent studies because it caused a clear spectral band to appear, which was thought to be the optimal condition, and reduced reaction kinetics and an inadequate nucleation rate at temperatures below pH could be to blame for the slow decline in peak intensity. To achieve the desired concentration of the bio-reductant, the copper salt solution was subsequently treated with varying volumes of CES additions, ranging from 1 millilitre to 5 millilitres. The next step was to bring the solution's pH down to 11. The CES was responsible for the significant drop that occurred with higher doses. A more favourable reduction and an elevated nucleation rate were the outcomes of increasing the quantity of reductant, which improved the reaction kinetics. Consequently, there were more discernible peaks in the UV-vis spectra. When four millilitres of CES was utilized as the assessment volume, the copper peak with the greatest amount of absorption was shown to be the most significant. A decrease in absorption intensity accompanied by an increase in CES might be due, in part, to the larger particle size. Once produced, nanoparticles will attempt to aggregate in a way that lowers their surface energy. According to (Khan et al., 2018), when there is an excess of bio-reductant, newly generated nuclei interact with pre-existing CuNPs, leading to an increase in particle size. Because of this contact, the size of the particles increases.

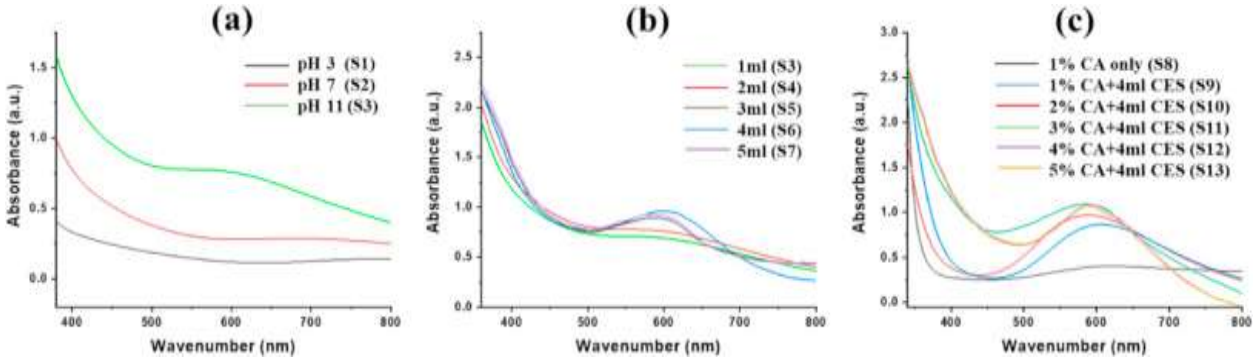

Fig.2. Illustrates how pH, CES concentration, and citric acid are shown to affect the UV absorption spectra.

(Beheshti et al., 2024) state that terpenoids, which are plant extracts containing isoprene, play a key role in converting metal salts to metal nanoparticles. Terpenoids are quite efficient in this kind of reduction. In cinnamon bark, you may find eugenol metabolites, which are a kind of terpenoid. Deprotonation of the hydroxyl group in eugenol is believed to lead to the formation of metal nanoparticles ultimately. An anionic population is formed when the proton is liberated during the deprotonation of the hydroxyl group. After the capping procedure, eugenol was proven to be a potent reducing agent by both (Theivasanthi & Alagar, 2012). This might be because the molecule contains strong electron-withdrawing groups in the ortho and para positions relative to the OH group, such as methyl and allyl. The molecule undergoes further oxidation and becomes a capping agent as a result. (Al-Yasiri & Wen, 2019) state that eugenol's reductive activity process is thermodynamically viable because its reduction potential is about -1.5 V, which is much lower than copper's reduction potential of about 0.34 V. Figure 3 shows the suggested approach of lowering and controlling the eugenol concentration.

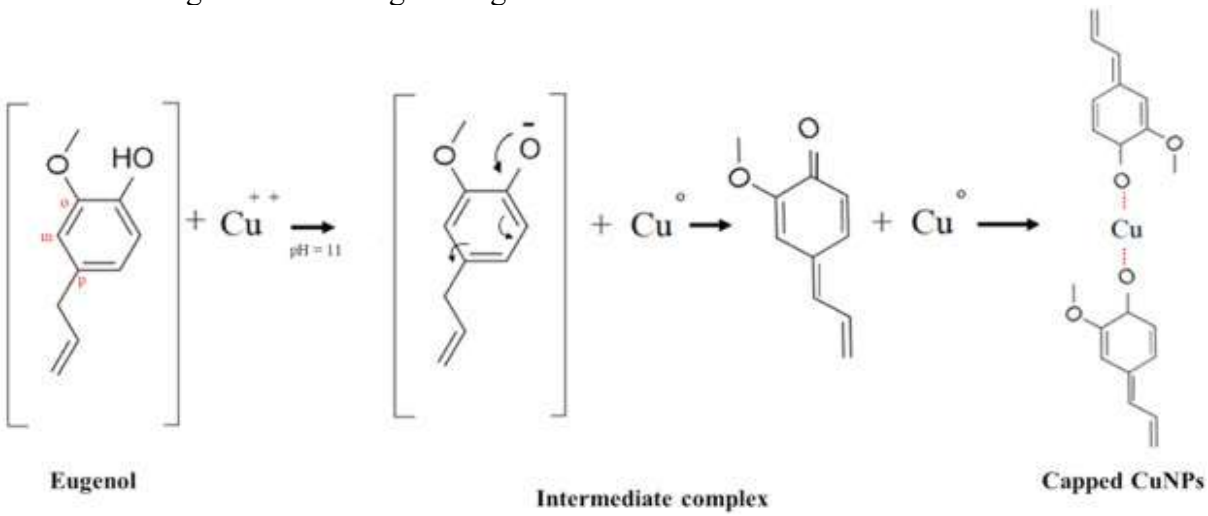

Fig.3. The capping procedure follows the eugenol reduction process.

3.2. Effect of citric acid

Numerous studies have investigated the antioxidant properties of citric acid, its role as a capping and stabilizing agent, and its low acidity (Imran Din & Rani, 2016) Three different amounts of citric acid, ranging from one to five per cent of the total volume, were added to the reaction medium to study its influence on the creation of copper nanoparticles (Table 2). Citric acid enhances cinnamon's reducing action, which accelerates the process and allows it to be completed more rapidly (Mao et al., 2015). Figure 2c shows that at a carcinogenic activity level of 4%, the UV-Vis spectra exhibited noticeably more intense

peaks. Citric acid is an antioxidant and free radical scavenger; when combined with cinnamon, it is believed to enhance its effects by drastically reducing copper salts. The findings of (Capasso et al., 2014) support this idea. The copper nanoparticles reached the brick-red hue seen in Figure 1c after twenty-five minutes of uniform dispersion.

3.3 SEM

The surface morphology of nanoparticles generated through biological activities was examined using field-emission scanning electron microscopy (FESEM), as shown in Figure 4. As seen in Figures 4a and 4b, the copper nanoparticles synthesized from citric acid exhibited a consistent spherical shape and a uniform surface roughness. Figure 4c and 4d show that the CuNPs made without CA were not uniformly distributed due to their shape and surface roughness. Cinnamon reduction occurs in a perfect environment created by citric acid's robust free radical scavenging capabilities, as shown in Figure 4a and Figure 4b. Jiang et al. (2010) also found that citrated ion radial adsorption onto CuNP surfaces may make the particles more homogeneous in shape. Both of these factors could explain why cinnamon levels have dropped. Copper makes up a significant portion of the material, according to the Energy Dispersive X-ray (EDX) spectra shown in Figure 4e. Since the strongest copper peaks occur at 1.00 keV and 8.00 keV, it follows that copper makes up approximately 84.70% of the substances mass. The interaction between the nanoparticles, bark extract, and citric acid may have reduced the visibility of the oxygen and carbon peaks.

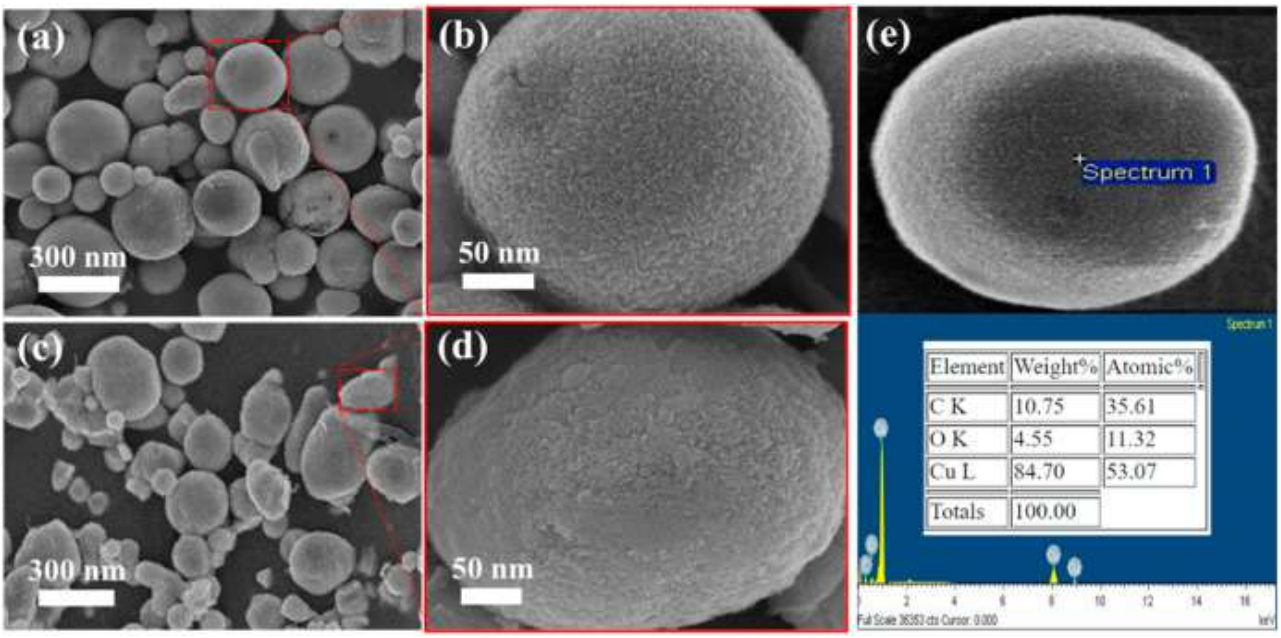

Fig.4. Scanning electron micrographs (SEM) of three distinct biosynthesized CuNP samples. The EDX spectra of S12 are shown in (a) through (b) and (c) through (d) here, and the samples consist of CES-S12 with citric acid mediation and S6 without mediation.

3.4. The X-ray diffraction findings

A method that is finding increasing applications in the field of crystal structure analysis and phase determination is powder X-ray diffraction. An XRD pattern shows copper nanoparticles biosynthesized from citric acid and CES. To see this pattern in action, refer to Figure 5. The presence of distinct peaks in

the pattern indicates the existence of a face-centred cubic structure, which is free from impurities and significant oxidation. These peaks correspond to 2θ values of 43.4°, 50.6°, and 74.2 °. The copper standard JCPDS No. 01-085-1326 seems to be in excellent alignment with the peaks seen at 43.4 degrees, 50.6 degrees, and 74.2 degrees. The (111), (200), and (220) peaks on the copper atomic structure are proportional to the respective planes. The lowest standard deviation might be due to surface capping and particle size dispersion, whereas the little peak at 39.05 degrees from the horizontal could be caused by surface oxidation.

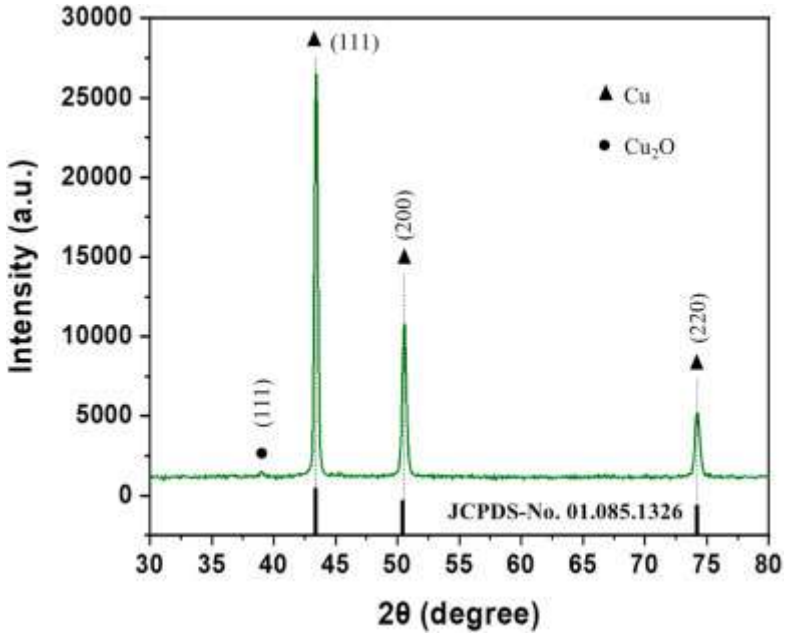

Fig.5. Shows the XRD spectrum of CuNPs obtained by biosynthesis using citric acid as a mediator.

3.5. Three-Fourier Transform Infrared Spectroscopy system

See Figure 6 for an example of the typical FTIR absorption spectra of cinnamon extract and CuNPs. According to the research done by (Gökdere et al., 2019), the main alcohols in eugenol are responsible for the large band seen at a frequency of 1012 cm−1. In the CES spectrum, several features are observed at 1510 cm−1 and 1615 cm−1. Eugenol is the biomolecule responsible for controlling the reduction process. The wide absorption band, with peaks between 3200 and 3500 cm−1, indicates the existence of -OH groups, which are accountable for the nanoparticle capping in the extract metabolites. The Fourier transform infrared (FTIR) spectra of biosynthesized copper nanoparticles (CuNPs) (samples S6 and S12, Table 2) show that the nanoparticles were functionalized during synthesis with biomolecules, as evidenced by the presence of peaks at 1663 cm−1 and 2960 cm−1, respectively, which correspond to the -C=O and -C=C functional groups. The presence of citric acid appears to have enhanced the nanoparticle capping process, as indicated by the strong -C=O and -C=C absorption bands in sample S12. The appearance of a band at 1712 cm−1 indicates the stretching of the C=C bond, which is caused by sample S12's surface absorption of citrate.

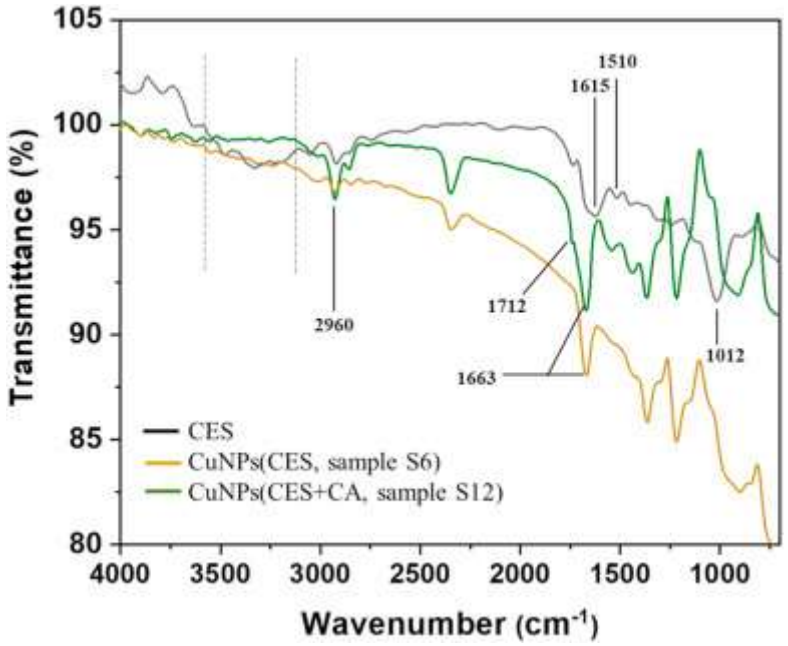

Fig.6. Displays the FTIR spectra of CuNPs and CES, regardless of whether citric acid is added or not

3.6. Methods that break down dyes via catalytic processes

Many people believe that organic dyes, which are naturally derived and considered toxic, are primarily responsible for water contamination. These hues are used in various sectors, including textiles, leather, and polymers. Traditional techniques, including filtration, adsorption, and electrochemical procedures, struggle to degrade or eliminate these hues from water (Bhuvaneshwari et al., 2024). This is because these colours last for a very long time. One advantage of biologically generated transition metal nanoparticles for the catalytic degradation of organic dyes is the enhanced functionality they confer via the adsorption of bioactive phytochemicals on their surfaces. Several investigations have been conducted on the reduction of MO and MB borohydrides using various metal nanoparticles (Narender et al., 2022). A great deal of work has been invested in these investigations. The investigations have yielded a plethora of new information. Biosynthesised metal nanoparticles lose some of their ecological integrity when a borohydride-based reducing agent is used, which can be harmful to the environment. The combination of boron hydroxide's solubility in water and its acute toxicity—which can lead to pulmonary oedema—makes diborane gas particularly lethal in acidic environments. The risks associated with borohydride have led to its classification as a hazardous substance under the Globally Harmonised System (GHS) (Ezhilarasi et al., 2020). Sodium hypophosphite is the term for the sodium salt that is present in concentrations of hypophosphorous acid. Paper, leather, and wood fibre production are just a few of the many industries that employ hypophosphite and its derivatives as bleaching agents (Din et al., 2018). The rationale for this is that salts are better reducing agents than their acid counterparts. The hypophosphite reduction of methylene blue and methyl orange was conducted using a milligram per litre of CuNPs, a very small amount, in order to assess the catalytic characteristics of the produced CuNPs. We did this so that we could determine the outcome of the experiment. The end outcome was that the potentially harmful SBH was successfully substituted with the safer SHP. This was preceded by adding 20 millilitres of a 50 parts

per million (ppm) dye solution to a 100 millilitre flask. Later, 20 milligrams of SHP per litre was added, and the mixture was mixed vigorously with and without nanoparticles, respectively. The catalytic breakdown of the dye near the nanoparticles of the substance is significantly affected by pH due to its influence on the adsorption rate. The experiment was conducted at three different pH levels — 3, 7, and 10 — to determine the degradation of the dye under acidic, neutral, and basic conditions. The findings of this experiment are shown in Table S1, which can be seen here. Both eye inspection and analysis of UV absorption spectra confirmed that the dye solution had been decolorized. To calculate the obtained degradation percentage, a standard concentration curve was created using Equation 1.

$$\%\mathbf{Degradation} = 100\text{x}\frac{\text{Ci}-\text{Cf}}{\text{Ci}} \quad \textbf{(1)}$$

Whereas Cf is the concentration of the dye solution after treatment, Ci is the concentration of the dye solution before usage.

The occurrence of a unique band at 460 nm in the anionic azo dye methyl orange is attributed, according to (Malligavathy & Pathinettam Padiyan, 2021), to the π-π transition of the azo group. Dye creates the illusion of this band. The addition of SHP alone did not cause any signs of color degradation, as reported by (Fujimoto et al., 2021). A discoloration was observed when the pH level reached 3, which is considered relatively high. Figure 7a shows that the addition of CuNPs resulted in a significant reduction of the absorption spectra, indicating that the particles exhibited effective catalytic activity. The adsorption of organic pollutants onto the catalyst surface is crucial for the degradation of dyes, according to (Medhi et al., 2020). When an anionic dye was more adsorbed to the surface of MO in an acidic solution, (Ali et al., 2022) found that MO broke down at a pH of 3. However, the dye's adhesion was diminished and its full absorption was hindered by ionic repulsion under acidic conditions.

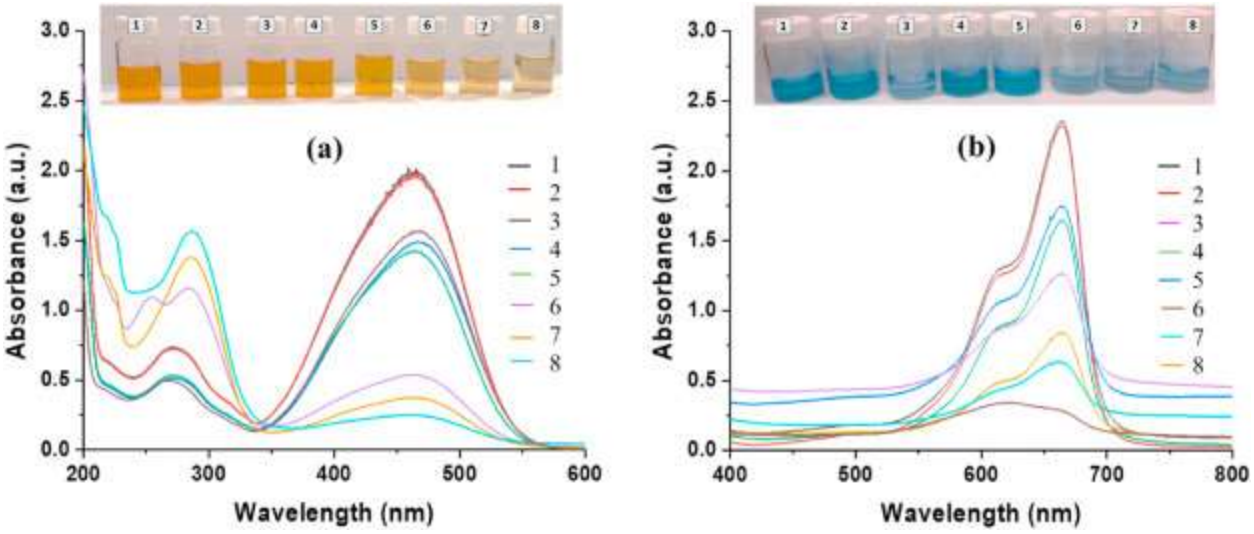

Fig.7. Displays the ultraviolet (UV) absorption spectra of methylene blue and methyl orange. Spectra show how SHP dyes degrade in the presence and absence of bio-produced CuNPs. For pH levels of 10, (a) untreated dye, (b) dye with CuNPs, and (c) dye with SHP. As a potential fourth choice, SHP has a pH of 7 and a dye number of 5. Bringing the pH of SHP up to three will allow it to absorb color. Dye, SHP, and CuNPs at the specified concentrations should be employed at a pH

of ten (pH=7). When the mixture reaches a pH of 3, include the dye, SHP, and CuNPs. Reducing the pH to a range of 3 is necessary.

Fabrics such as cotton, wool, and silk have been colored with methylene blue, a cationic heterocyclic thiazine dye, for quite some time. This approach has been extensively used for a long period. The breakdown of MB releases many aromatic amines into the atmosphere, some of which are recognized carcinogens. Amines such as benzidine and methylene are among them. Those who care about environmental preservation see it as a major issue. Degradation of MB was more efficient at an alkaline pH; all of the generated CuNPs had similar efficacy (Fig. 7b). The acidity of the surface became more noticeably negative as a result of the surrounding environment's pH increasing. (Jeon et al., 2018) found that MB is easily adsorbed onto the surface of catalytic CuNPs in environments with an alkaline Ph. This occurs because MB is cationic, which means it accelerates the degradation process that the catalyst is carrying out. Figure 8 displays the fraction of deterioration suffered by MO and MB, derived from their respective calibration curves, as shown in Figure S1.

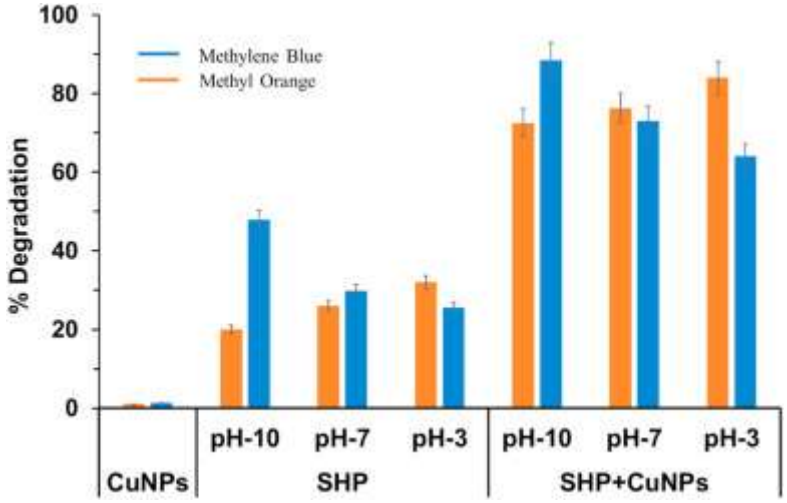

Fig.8. Displays the results of a dye degradation measurement made using the STD calibration curve.

When metal nanoparticles are present, sodium hypophosphite, like sodium borohydride (SBH), donates electrons, facilitating the catalytic reduction of MO and MB colorants. The research of (Fardood et al., 2024) supports this idea. Copper nanoparticles facilitate the transfer of electrons from the hypophosphite ion to the dye by acting as a conduit during the color degradation process. According to research by (Farghali et al., 2019), H2PO2 is the one that initiates the transfer of electrons to copper nanoparticles when they are in proximity to each other. At the end of this process, a coating of negatively charged material will have formed around the nuclear particles. This layer may be easily transferred to the dyestuff, allowing for a reduction in production volume.

3.7. Antimicrobial performance

Applying the technology, the antibacterial efficacy of the as-synthesized CuNPs was evaluated using the disc diffusion method. The microorganisms that were examined were Staphylococcus aureus and Escherichia coli samples. Acid mutagen mitigation was included in the evaluation process and was also

tested independently. Both the nutritional agar and the Luria-Bertani (LB) broth were produced in deionized water and then autoclaved once each component had reached a concentration of twenty grams per liter. The process of creating a uniform bacterial inoculum began by picking a single colony, which was then transferred to LB Broth solution and incubated at 37°C for 6 hours. The inoculum was acquired six hours later by diluting it with LB broth, which produced a bacterial inoculum with an optical density (OD) of 0.5. The inoculum was then used to plant the bacterial seeds that would later grow into the test culture. Before beginning the experiment, a previously sterilized Petri dish was filled with 25 milliliters of nutritious agar solution and left to solidify for a specified amount of time. The next step was to uniformly streak the bacterial culture at an optical density of 0.5. After the discs were removed from the 100% cotton fabric, they were treated with a CuNP solution at a concentration of 1 milligram per milliliter (Table S2). The discs were set on the solidified medium after being air-dried and cured at 160 degrees Celsius for 90 seconds. The inhibitory zone of the setup was tested after 24 hours of incubation at 37°C (Table 3). Inhibitory zones were not seen in the untreated samples that were attacked by microbes. Research by (Mohammadi et al., 2023) demonstrated that copper nanoparticles exhibit antibacterial properties due to their ability to interact with bacterial cells through the thiol groups of proteins. Staphylococcus aureus and Escherichia coli were both killed by the "A" and "B" samples, respectively. The inhibitory zone analysis showed that the bacterial suspension was much improved in Sample B, which included citric acid-mediated CuNPs. Figure 9 clearly shows this proof. Surface roughness of the CA-mediated CuNPs in sample "B" is similar to that of a cactus ball. Figure 4b illustrates that the outcome is an increase in the activity of the bacterial solution, accompanied by a high surface-to-volume ratio. The innate antibacterial properties of citric acid may enhance the effectiveness of nanoparticles, as demonstrated by a 2019 study by (Agi et al., 2022).

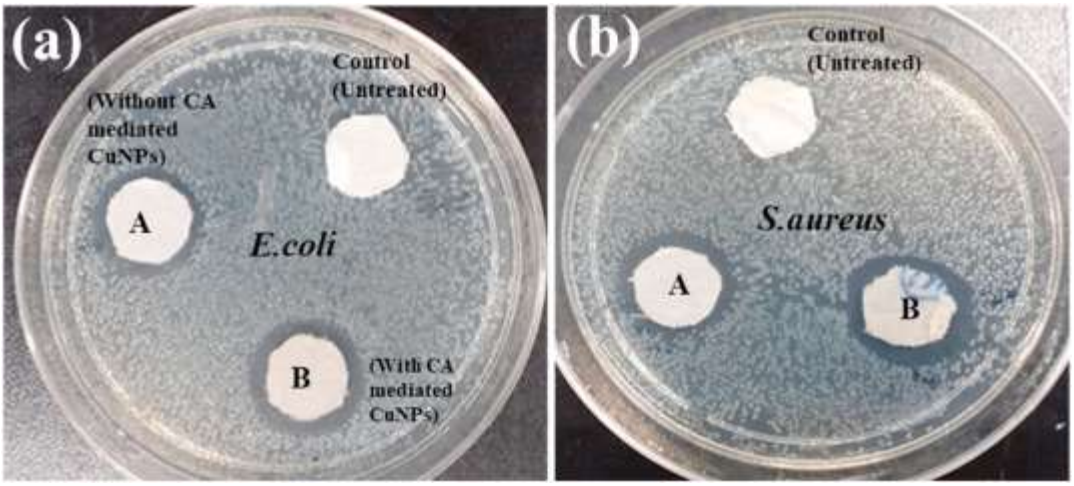

Fig. 9. Photographs of the antimicrobial test discs: (a) E. coli; (b) S. aureus.

Table 3. Suppression zone of treated cloth against Staphylococcus aureus and Escherichia coli.

Sample ID	Description	Inhibition zone (mm)	
		S. aureus	E. coli
Control	Untreated	0	0
A	Padded with CuNPs synthesized using cinnamon only.	21	19
B	Padded with CuNPs synthesized using cinnamon and citric acid.	28	23

4. Conclusion

The present study successfully demonstrated an environmentally benign and efficient method for synthesizing copper nanoparticles (CuNPs) through a citric acid-mediated biosynthetic route using cinnamon bark extract. The approach addresses the limitations of conventional chemical synthesis routes, which often rely on toxic reductants and stabilizers, by harnessing the reducing potential of cinnamon phytochemicals while utilizing citric acid as a mediator to enhance the reduction process and control nanoparticle morphology. This synergistic combination proved effective in overcoming the inadequate reduction capacity of natural extracts alone, yielding uniformly distributed, spherical nanoparticles with consistent surface roughness. Comprehensive characterization using UV–Vis spectroscopy, SEM, XRD, and FTIR confirmed the crystalline structure, stability, and biomolecule-assisted capping of the synthesized CuNPs, reinforcing the reliability of the method.

Functionally, the biosynthesized CuNPs exhibited remarkable catalytic potential. In dye degradation studies, the nanoparticles achieved over 80% removal efficiency against carcinogenic dyes such as methylene blue (MB) and methyl orange (MO) when used in combination with sodium hypophosphite, a non-toxic reducing agent. This performance highlights their suitability as catalysts for wastewater treatment, addressing the urgent need for sustainable strategies to mitigate environmental pollution caused by synthetic dyes. The catalytic efficiency, achieved under mild conditions, further underscores the economic and ecological viability of this green synthesis approach.

In addition to their catalytic activity, the CuNPs displayed significant antibacterial properties. Disc diffusion assays against Staphylococcus aureus and Escherichia coli revealed strong inhibitory effects, with citric acid-mediated CuNPs producing larger inhibition zones compared to nanoparticles synthesized with cinnamon alone. This enhanced antibacterial performance can be attributed to the improved surface morphology and higher surface-to-volume ratio imparted by citric acid mediation, as well as the intrinsic antimicrobial properties of both copper and citric acid. The results indicate that these nanoparticles could be effectively integrated into antimicrobial textiles, coatings, medical fabrics, and personal protective equipment, offering broad-spectrum protection against pathogenic microorganisms.

The novelty of this study lies not only in the successful use of cinnamon bark extract for CuNP synthesis but also in demonstrating the dual role of citric acid as both a mediator and functional enhancer. By accelerating the reduction kinetics and providing stabilization, citric acid contributed to the reproducibility, scalability, and performance of the final product. This represents a significant step forward

in advancing biosynthetic nanoparticle production, which has historically been limited by inconsistent particle distribution and weak reduction efficiencies.

From a broader perspective, this research contributes to the growing field of sustainable nanotechnology by offering a simple, low-cost, and eco-friendly approach that eliminates the use of hazardous chemicals. The method is adaptable, energy-efficient, and compatible with large-scale production, making it relevant not only for laboratory research but also for industrial implementation. The multifunctional properties of the synthesized CuNPs—catalytic, antibacterial, and structurally stable—position them as promising candidates for applications in wastewater management, biomedical textiles, antimicrobial packaging, and potentially in addressing public health crises such as pandemics.

Despite these promising outcomes, further studies are recommended to expand the scope of this research. Future work should investigate the long-term stability of nanoparticles under various environmental conditions, their cytotoxicity and biocompatibility for safe biomedical applications, and their reusability in catalytic systems to assess cost-effectiveness in industrial-scale processes. Additionally, exploring other plant extracts in combination with citric acid could broaden the library of green synthesis strategies and yield nanoparticles with tailored properties for specific applications.

In conclusion, the study demonstrates that the citric acid-mediated biosynthesis of copper nanoparticles using cinnamon bark extract is a viable, sustainable, and multifunctional approach. The synthesized CuNPs not only deliver outstanding catalytic and antibacterial performance but also align with the principles of green chemistry and circular economy. By bridging the gap between nanotechnology, environmental sustainability, and practical applications, this research lays the foundation for developing advanced nanomaterial’s that can contribute to addressing pressing biomedical and ecological challenges.

References

Abdo, J., & Haneef, M. D. (2013). Clay nanoparticles modified drilling fluids for drilling of deep hydrocarbon wells. Applied Clay Science, 86, 76–82.

Aftab, A., Ali, M., Sahito, M. F., Mohanty, U. S., Jha, N. K., Akhondzadeh, H., Azhar, M. R., Ismail, A. R., Keshavarz, A., & Iglauer, S. (2020). Environmental friendliness and high performance of multifunctional tween 80/ZnO-nanoparticles-added water-based drilling fluid: an experimental approach. ACS Sustainable Chemistry & Engineering, 8(30), 11224–11243.

Agi, A., Junin, R., Jaafar, M. Z., Amin, N. A. S., Sidek, M. A., Yakasai, F., Faizal, A. N. M., Gbadamosi, A., & Oseh, J. (2022). Process optimization of reservoir fines trapping by mesoporous silica nanoparticles using Box-Behnken design. Alexandria Engineering Journal, 61(11), 8809–8821.

Ahamed, M., Ali, D., Alhadlaq, H. A., & Akhtar, M. J. (2013). Nickel oxide nanoparticles exert cytotoxicity via oxidative stress and induce apoptotic response in human liver cells (HepG2). Chemosphere, 93(10), 2514–2522.

Ahmad, H. M., Iqbal, T., Al Harthi, M. A., & Kamal, M. S. (2021). Synergistic effect of polymer and nanoparticles on shale hydration and swelling performance of drilling fluids. Journal of Petroleum Science and Engineering, 205, 108763.

Al-Yasiri, M., & Wen, D. (2019). Gr-Al2O3 Nanoparticles-based multifunctional drilling fluid. Industrial & Engineering Chemistry Research, 58(23), 10084–10091.

Ali, T., Warsi, M. F., Zulfiqar, S., Sami, A., Ullah, S., Rasheed, A., Alsafari, I. A., Agboola, P. O., Shakir, I., & Baig, M. M. (2022). Green nickel/nickel oxide nanoparticles for prospective antibacterial and environmental remediation applications. Ceramics International, 48(6), 8331–8340.

Almomani, F., Bhosale, R., Khraisheh, M., Kumar, A., & Tawalbeh, M. (2020). Electrochemical oxidation of ammonia on nickel oxide nanoparticles. International Journal of Hydrogen Energy, 45(17), 10398–10408.

Anand, G. T., Nithiyavathi, R., Ramesh, R., Sundaram, S. J., & Kaviyarasu, K. (2020). Structural and optical properties of nickel oxide nanoparticles: Investigation of antimicrobial applications. Surfaces and Interfaces, 18, 100460.

Anitha Devi, S., Reddy, G. R., Srinivasa Rao, M., Nagarjuna, C., Kolenčík, M., Ramakanth, I., Joo, S. W., & Madhavi, G. (2025). Titanium dioxide nanoparticles-decorated reduced graphene oxide for highly sensitive electrochemical detection of chloramphenicol. Microchemical Journal, 213, 113717. https://doi.org/https://doi.org/10.1016/j.microc.2025.113717

Aramendiz, J., & Imqam, A. (2019). Water-based drilling fluid formulation using silica and graphene nanoparticles for unconventional shale applications. Journal of Petroleum Science and Engineering, 179, 742–749.

Arumugam, C., Velu, N., Radhakrishnan, P., Roy, V. A. L., Anantha-Iyengar, G., Lee, D.-E., & Kannan,

V. (2023). Studies on the functional properties of titanium dioxide nanoparticles distributed in silyl–alkyl bridged polyaniline-based nanofluids. Nanomaterials, 13(16), 2332.

Baghirova, L., Kaya Tilki, E., & Ozturk, A. A. (2023). Evaluation of Cell Proliferation and Wound Healing Effects of Vitamin A Palmitate-Loaded PLGA/Chitosan-Coated PLGA Nanoparticles: Preparation, Characterization, Release, and Release Kinetics. ACS Omega, 8(2), 2658–2668.

Beheshti, A. K., Rezaei, M., Alavi, S. M., Akbari, E., & Varbar, M. (2024). Enhanced performance and recyclability of cobalt nanoparticles mesoporous Catalyst supported on mechanochemically prepared CoFe2O4–Co3O4 for sodium borohydride hydrolysis. International Journal of Hydrogen Energy, 93, 1156–1165. https://doi.org/https://doi.org/10.1016/j.ijhydene.2024.11.019

Benelmekki, M., Vernieres, J., Kim, J.-H., Diaz, R.-E., Grammatikopoulos, P., & Sowwan, M. (2015). On the formation of ternary metallic-dielectric multicore-shell nanoparticles by inert-gas condensation method. Materials Chemistry and Physics, 151, 275–281.

Bhuvaneshwari, N., Arulmathi, M., Venkatesh, R., BoopathiRaja, R., Al-lohedan, H., Balu, R., & Parthibavarman, M. (2024). Green synthesis of Zn-doped NiFe2O4 nanoparticles using Hibiscus rosa-sinensis leaf extract: optical, photocatalytic, and antioxidant properties. Journal of Materials Science: Materials in Electronics, 35(11), 782.

Capasso, L., Camatini, M., & Gualtieri, M. (2014). Nickel oxide nanoparticles induce inflammation and genotoxic effect in lung epithelial cells. Toxicology Letters, 226(1), 28–34.

Cheraghian, G. (2021). Nanoparticles in drilling fluid: A review of the state-of-the-art. Journal of Materials Research and Technology, 13, 737–753.

Cheraghian, G., Hemmati, M., & Bazgir, S. (2014). Application of TiO 2 and fumed silica nanoparticles and improve the performance of drilling fluids. AIP Conference Proceedings, 1590(1), 266–270.

Din, M. I., Nabi, A. G., Rani, A., Aihetasham, A., & Mukhtar, M. (2018). Single step green synthesis of stable nickel and nickel oxide nanoparticles from Calotropis gigantea: catalytic and antimicrobial potentials. Environmental Nanotechnology, Monitoring & Management, 9, 29–36.

Esa, Y. A. M., & Sapawe, N. (2020). A short review on zinc metal nanoparticles synthesize by green chemistry via natural plant extracts. Materials Today: Proceedings, 31, 386–393.

Ezhilarasi, A. A., Vijaya, J. J., Kaviyarasu, K., Zhang, X., & Kennedy, L. J. (2020). Green synthesis of nickel oxide nanoparticles using Solanum trilobatum extract for cytotoxicity, antibacterial and photocatalytic studies. Surfaces and Interfaces, 20, 100553.

Fardood, S. T., Moradnia, F., Ganjkhanlu, S., Ouni, L., Ramazani, A., & Sillanpää, M. (2024). Green synthesis and characterization of spinel CoAl2O4 nanoparticles: Efficient photocatalytic degradation of organic dyes. Inorganic Chemistry Communications, 112719.

Farghali, M., Andriamanohiarisoamanana, F. J., Ahmed, M. M., Kotb, S., Yamashiro, T., Iwasaki, M., & Umetsu, K. (2019). Impacts of iron oxide and titanium dioxide nanoparticles on biogas production:

Hydrogen sulfide mitigation, process stability, and prospective challenges. Journal of Environmental Management, 240, 160–167. https://doi.org/https://doi.org/10.1016/j.jenvman.2019.03.089

Fujimoto, M., Matsumoto, M., Nagatsuka, N., & Fukutani, K. (2021). Blackening of titanium dioxide nanoparticles by atomic hydrogen and the effect of coexistence of water on the blackening. RSC Advances, 11(7), 4270–4275. https://doi.org/https://doi.org/10.1039/d0ra09090e

Gbadamosi, A., Yusuff, A., Agi, A., Muruga, P., Junin, R., & Jeffrey, O. (2022). Mechanistic study of nanoparticles-assisted xanthan gum polymer flooding for enhanced oil recovery: A comparative study. Journal of Petroleum Exploration and Production Technology, 1–7.

Gökdere, B., Üzer, A., Durmazel, S., Erçağ, E., & Apak, R. (2019). Titanium dioxide nanoparticles–based colorimetric sensors for determination of hydrogen peroxide and triacetone triperoxide (TATP). Talanta, 202, 402–410. https://doi.org/https://doi.org/10.1016/j.talanta.2019.04.071

Green, M., Van Tran, A. T., Smedley, R., Roach, A., Murowchick, J., & Chen, X. (2019). Microwave absorption of magnesium/hydrogen-treated titanium dioxide nanoparticles. Nano Materials Science, 1(1), 48–59. https://doi.org/https://doi.org/10.1016/j.nanoms.2019.02.001

Gui, H., Liu, H., Cai, Y., Nian, J., Liu, L., Song, Y., Kye, S., Zuo, S., & Yao, C. (2025). Hyaluronic acid-grafted titanium dioxide nanoparticles for moisture-retentive and non-cytotoxic sunscreen creams. International Journal of Biological Macromolecules, 311, 143957. https://doi.org/https://doi.org/10.1016/j.ijbiomac.2025.143957

Huang, X., Lv, K., Sun, J., Lu, Z., Bai, Y., Shen, H., & Wang, J. (2019). Enhancement of thermal stability of drilling fluid using laponite nanoparticles under extreme temperature conditions. Materials Letters, 248, 146–149.

Imran Din, M., & Rani, A. (2016). Recent advances in the synthesis and stabilization of nickel and nickel oxide nanoparticles: a green adeptness. International Journal of Analytical Chemistry, 2016(1), 3512145.

Jahanbakhshi, M., & Habibi, B. (2016). A novel and facile synthesis of carbon quantum dots via salep hydrothermal treatment as the silver nanoparticles support: Application to electroanalytical determination of H2O2 in fetal bovine serum. Biosensors and Bioelectronics, 81, 143–150.

Jeon, B.-H., Yang, D.-H., Kim, Y.-D., Shin, J. S., & Lee, C.-S. (2018). Fabrication of silver nanoparticles in titanium dioxide/poly(vinyl alcohol) alternate thin films: A nonenzymatic hydrogen peroxide sensor application. Electrochimica Acta, 292, 749–758. https://doi.org/https://doi.org/10.1016/j.electacta.2018.08.125

Justo-Vega, A., Vázquez-Pérez, S., Domínguez-González, R., Bermejo-Barrera, P., & Moreda-Piñeiro, A. (2025). Enzymatic hydrolysis for pre-treating human serum before titanium dioxide nanoparticles assessment by spICP-MS. Talanta, 291, 127766. https://doi.org/https://doi.org/10.1016/j.talanta.2025.127766

Kavitha, R., Veni, K. K., Sagadevan, S., & Nehru, L. C. (2024). Enhanced visible light-driven

photocatalytic activity of green synthesized cobalt ferrite nanoparticles. Ceramics International, 50(3), 4861–4874.

Khan, M. A., Al-Salim, H. S., & Arsanjani, L. N. (2018). Development of high temperature high pressure (HTHP) water based drilling mud using synthetic polymers, and nanoparticles. Journal of Advanced Research in Fluid Mechanics and Thermal Sciences, 45(1), 99–108.

Khoiriah, K., & Putri, R. A. (2024). Biosynthesis of titanium dioxide nanoparticles using peel extract of Parkia speciosa for methyl orange degradation. South African Journal of Botany, 170, 120–129. https://doi.org/https://doi.org/10.1016/j.sajb.2024.05.021

Kotb, E., & M. Alabdallah, N. (2024). Chapter eleven - Function of nanoparticles as nanozymes in biochemical reactions and their environmental and biomedical applications. In H. Tombuloglu, G. Tombuloglu, E. Al-Suhaimi, A. Baykal, & K. R. Hakeem (Eds.), Molecular Impacts of Nanoparticles on Plants and Algae (pp. 211–248). Academic Press. https://doi.org/https://doi.org/10.1016/B978-0-323-95721-2.00014-2

Lashari, N., Ganat, T., Elraies, K. A., Ayoub, M. A., Kalam, S., Chandio, T. A., Qureshi, S., & Sharma, T. (2022). Impact of nanoparticles stability on rheology, interfacial tension, and wettability in chemical enhanced oil recovery: A critical parametric review. Journal of Petroleum Science and Engineering, 212, 110199.

Li, F., Li, J., Chen, L., Dong, Y., Xie, P., & Li, Q. (2021). Preparation of CoB nanoparticles decorated PANI nanotubes as catalysts for hydrogen generation from NaBH4 hydrolysis. Journal of the Taiwan Institute of Chemical Engineers, 122, 148–156.

Li, M.-C., Wu, Q., Song, K., Qing, Y., & Wu, Y. (2015). Cellulose nanoparticles as modifiers for rheology and fluid loss in bentonite water-based fluids. ACS Applied Materials & Interfaces, 7(8), 5006–5016.

Liu, X., Liu, Z., Lu, J., Wu, X., & Chu, W. (2014). Silver sulfide nanoparticles sensitized titanium dioxide nanotube arrays synthesized by in situ sulfurization for photocatalytic hydrogen production. Journal of Colloid and Interface Science, 413, 17–23. https://doi.org/https://doi.org/10.1016/j.jcis.2013.09.031

Luo, Q., Liu, X., Xu, Q., Tian, Y., Yao, H., Wang, J., Lv, S., Dang, C., & Xuan, Y. (2023). Ceramic nanoparticles enhancement of latent heat thermal energy storage properties for LiNO3/NaCl: Evaluation from material to system level. Applied Energy, 331. https://doi.org/10.1016/J.APENERGY.2022.120418

Madadkhani, S., Nandy, S., Aleshkevych, P., Chae, K. H., Allakhverdiev, S. I., & Najafpour, M. M. (2024). Decomposition of a manganese complex loaded on TiO2 nanoparticles under photochemical reaction. International Journal of Hydrogen Energy, 51, 742–746. https://doi.org/https://doi.org/10.1016/j.ijhydene.2023.10.196

Malligavathy, M., & Pathinettam Padiyan, D. (2021). Role of pH in the hydrothermal synthesis of phase pure alpha Bi2O3 nanoparticles and its structural characterization. Advanced Materials Proceedings, 2(1), 51–55. https://doi.org/10.5185/amp.2017/112

Mao, H., Qiu, Z., Shen, Z., & Huang, W. (2015). Hydrophobic associated polymer based silica nanoparticles composite with core–shell structure as a filtrate reducer for drilling fluid at utra-high temperature. Journal of Petroleum Science and Engineering, 129, 1–14.

Mathew, D. S., & Juang, R.-S. (2007). An overview of the structure and magnetism of spinel ferrite nanoparticles and their synthesis in microemulsions. Chemical Engineering Journal, 129(1–3), 51–65.

Medhi, S., Chowdhury, S., Gupta, D. K., & Mazumdar, A. (2020). An investigation on the effects of silica and copper oxide nanoparticles on rheological and fluid loss property of drilling fluids. Journal of Petroleum Exploration and Production Technology, 10(1), 91–101.

Mishra, S., Dalai, R., & Swain, K. (2023). Effects of copper and titania nanoparticles on MHD 3D rotational flow over an elongating sheet with convective thermal boundary condition. International Journal of Ambient Energy, 44(1), 381–389.

Mohammadi, T., Asadpour-Zeynali, K., Majidi, M. R., & Hosseini, M. G. (2023). Ru–Ni nanoparticles electrodeposited on rGO/Ni foam as a binder-free, stable and high-performance anode catalyst for direct hydrazine fuel cell. Heliyon, 9(6), e16888. https://doi.org/https://doi.org/10.1016/j.heliyon.2023.e16888

Moshirian Farahi, S. M., Taghavizadeh Yazdi, M. E., Einafshar, E., Akhondi, M., Ebadi, M., Azimipour, S., Mahmoodzadeh, H., & Iranbakhsh, A. (2023). The effects of titanium dioxide (TiO2) nanoparticles on physiological, biochemical, and antioxidant properties of Vitex plant (Vitex agnus - Castus L). Heliyon, 9(11), e22144. https://doi.org/https://doi.org/10.1016/j.heliyon.2023.e22144

Muraro, P. C. L., Wouters, R. D., Druzian, D. M., Viana, A. R., Schuch, A. P., Rech, V. C., & da Silva, W. L. (2024). Ecotoxicity and in vitro safety profile of the eco-friendly silver and titanium dioxide nanoparticles. Process Safety and Environmental Protection, 188, 584–594. https://doi.org/https://doi.org/10.1016/j.psep.2024.05.151

Narender, S. S., Varma, V. V. S., Srikar, C. S., Ruchitha, J., Varma, P. A., & Praveen, B. V. S. (2022). Nickel oxide nanoparticles: a brief review of their synthesis, characterization, and applications. Chemical Engineering & Technology, 45(3), 397–409.

Nayak, B. B., Vitta, S., Nigam, A. K., & Bahadur, D. (2006). Ni and Ni–nickel oxide nanoparticles with different shapes and a core–shell structure. Thin Solid Films, 505(1–2), 109–112.

Needaa, A.-M., Pourafshary, P., Hamoud, A.-H., & Jamil, A. (2016). Controlling bentonite-based drilling mud properties using sepiolite nanoparticles. Petroleum Exploration and Development, 43(4), 717–723.

Noghabi, M. P., Parizadeh, M. R., Ghayour-Mobarhan, M., Taherzadeh, D., Hosseini, H. A., & Darroudi, M. (2017). Green synthesis of silver nanoparticles and investigation of their colorimetric sensing and cytotoxicity effects. Journal of Molecular Structure, 1146, 499–503.

Onwudiwe, D. C., Ravele, M. P., & Elemike, E. E. (2020). Eco-friendly synthesis, structural properties and morphology of cobalt hydroxide and cobalt oxide nanoparticles using extract of Litchi chinensis. Nano-Structures & Nano-Objects, 23, 100470.

Patade, S. R., Andhare, D. D., Somvanshi, S. B., Jadhav, S. A., Khedkar, M. V, & Jadhav, K. M. (2020). Self-heating evaluation of superparamagnetic MnFe2O4 nanoparticles for magnetic fluid hyperthermia application towards cancer treatment. Ceramics International, 46(16), 25576–25583.

Salgaokar, M. D. (2023). Effect of Rare-earth Doping on Structural, Magnetic and Electric Properties of Transition Metal Ferrite Nanoparticles. Goa University.

Sánchez-Tovar, M. R., Carvajal-Valenzuela, I. A., Godínez-Mendoza, P. L., Rivera-Bustamante, R. F., Saavedra-Trejo, D. L., Guevara-González, R. G., & Torres-Pacheco, I. (2025). Protective effects of titanium dioxide nanoparticles in Jalapeño chili pepper (Capsicum annuum L.) in a viral single and mixed infection study model. Physiological and Molecular Plant Pathology, 136, 102560. https://doi.org/https://doi.org/10.1016/j.pmpp.2024.102560

Singh, S., Bhatnagar, A., Shukla, V., Pandey, A. P., & Shaz, M. A. (2025). Three-dimensional graphene aerogel decorated with nickel nanoparticles as additive for improving the hydrogen storage properties of MgH2. International Journal of Hydrogen Energy, 107, 96–107. https://doi.org/https://doi.org/10.1016/j.ijhydene.2024.12.331

Swain, K., Ibrahim, S. M., Dharmaiah, G., & Noeiaghdam, S. (2023). Numerical study of nanoparticles aggregation on radiative 3D flow of maxwell fluid over a permeable stretching surface with thermal radiation and heat source/sink. Results in Engineering, 19, 101208.

Teo, S. H., Islam, A., Chan, E. S., Choong, S. Y. T., Alharthi, N. H., Taufiq-Yap, Y. H., & Awual, M. R. (2019). Efficient biodiesel production from Jatropha curcus using CaSO4/Fe2O3-SiO2 core-shell magnetic nanoparticles. Journal of Cleaner Production, 208, 816–826.

Theivasanthi, T., & Alagar, M. (2012). Chemical capping synthesis of nickel oxide nanoparticles and their characterizations studies. ArXiv Preprint ArXiv:1212.4595.

Vargas, J., Roldán, L. J., Lopera, S. H., Cardenas, J. C., Zabala, R. D., Franco, C. A., & Cortés, F. B. (2019). Effect of silica nanoparticles on thermal stability in bentonite free water-based drilling fluids to improve its rheological and filtration properties after aging process. Offshore Technology Conference Brasil, D011S007R003.

Wang, Q., Lin, S., Luo, H., Yu, W., Liu, W., Chen, F., & Cheng, D. (2024). Enhanced photocatalytic dehydrogenation of formic acid over ultrafine electron-deficient Pd nanoparticles immobilized on amine-functionalized mesoporous titanium dioxide. International Journal of Hydrogen Energy, 77, 1307–1316. https://doi.org/https://doi.org/10.1016/j.ijhydene.2024.06.226

Yan, Z., Wu, H., Han, A., Yu, X., & Du, P. (2014). Noble metal-free cobalt oxide (CoOx) nanoparticles loaded on titanium dioxide/cadmium sulfide composite for enhanced photocatalytic hydrogen production from water. International Journal of Hydrogen Energy, 39(25), 13353–13360. https://doi.org/https://doi.org/10.1016/j.ijhydene.2014.04.121

Zhang, Z., Tang, S., Xu, L., Wang, J., Li, A., Jing, M., Yang, X., & Song, F. (2024). Encapsulation of ruthenium oxide nanoparticles in nitrogen-doped porous carbon polyhedral for pH-universal hydrogen evolution electrocatalysis. International Journal of Hydrogen Energy, 74, 10–16.